Observation of Shubnikov–de Haas oscillations in the quasi-one-dimensional Bechgaard salt

$(TMTSF)_2FSO_3$

Observation of Shubnikov–de Haas oscillations in the quasi-one-dimensional Bechgaard salt (TMTSF)$_2$FSO$_3$

O H Chung[1,2]**, Y J Jo**[3]**, Haeyong Kang**[3] **and W Kang**[3]

[1] Department of Physics, Sunchon University, Suncheon 540-742, Korea
[2] National High Magnetic Field Laboratory, 1800 E Paul Dirac Drive, Tallahassee, FL 32306, USA
[3] Department of Physics, Ewha Womans University, Seoul 120-750, Korea

E-mail: ohchung@sunchon.ac.kr

Abstract
The longitudinal magnetoresistance of the unusual Bechgaard salt, (TMTSF)$_2$FSO$_3$, has been studied up to 33 T under various pressures. In this compound, a single series of the Shubnikov–de Haas (SdH) oscillation is very pronounced for pressures between 5.2 and 11.8 kbar where the zero-field ground state is superconducting. Unlike the case of the rapid oscillations in most Bechgaard salts, the temperature and magnetic field dependence of the oscillations is in good agreement with the Lifshitz–Kosevich formula, implying the two-dimensional closed orbital motion of the electrons. The effective mass of the electrons and Dingle temperature are estimated as $1.4 \pm 0.05\ m_0$ and 1.6–2.4 K, respectively. For an origin of the closed orbits, it is suggested that incomplete nesting between open Fermi surfaces is induced by pressure. Discontinuous change of the frequency, amplitude, and Dingle temperature of the oscillations around 9 kbar indicates that the electronic state below and above this pressure is different. According to the features of the SdH oscillations along with the phase diagram of (TMTSF)$_2$FSO$_3$, the pressure dependence is divided into three regions.

1. Introduction

The existence of a closed electron orbit on the Fermi surface (FS) is a necessary condition to observe Shubnikov–de Haas (SdH) oscillations in low-dimensional electron systems. Although the performance of a closed orbital electron motion is hard to envisage in (TMTSF)$_2$X (TMTSF = tetramethyltetraselenafulvalene and X = ClO$_4$, ReO$_4$, NO$_3$, PF$_6$, AsF$_6$, etc), which are primarily one-dimensional (1D) materials, two kinds of oscillations in the magnetoresistance have been observed in most Bechgaard salts [1–7]. The first series, known as slow oscillations ($F_0 \approx$ 20–70 T, where F_0 denotes the fundamental frequency), are successfully explained by a series of transitions of the field-induced spin-density-wave (FISDW) states according to the standard model [8, 9]. The second type of oscillations, so-called fast or rapid oscillations (ROs, $F_0 \approx$ 200–300 T), is very reminiscent of the conventional SdH oscillations from the viewpoint

of the fact that the oscillations are periodic in $1/H$ and their frequency depends on only the $\mathbf{c}^*$ component of the magnetic field. However, the unique temperature and field dependence of the ROs in the Bechgaard salts is inexplicable through the conventional Lifshitz–Kosevich (LK) analysis for typical closed orbital motions [10, 11]. The temperature dependence curve of the amplitude of the ROs shows a maximum around 3 K and the oscillations eventually vanish at very low temperature [12–15]. The field dependence of the amplitude also deviates from the Dingle reduction behaviour. Such anomalies of the ROs in the Bechgaard salts arise from their unique origin which is different from that in two-dimensional (2D) metals. It is generally accepted that the ROs originate from the magnetic breakdown of reconstructed, nested quasi-one-dimensional (Q1D) FS topology [13, 15], so application of the LK formula cannot account for the oscillations in the Bechgaard salts.

Moreover, symmetry and orientational ordering of anions play an important role in determining the properties of the ROs (number of series, frequency, etc). While a single series of ROs appear only in the SDW phase for the centrosymmetric anion salts [2–4], in the case of noncentrosymmetric anion salts they are observed both in the metallic and SDW phases [5, 6, 13]. The ROs in the metallic phase of $(TMTSF)_2ClO_4$ are attributed to the Stark quantum interference effect between two FS sheets where electrons proceed along the same direction, due to the anion ordering along the b-axis. Furthermore, the ROs in the SDW phase exhibit even more complicated behaviour, such as two out-of-phase series oscillations with the same frequency in ClO_4 salt [14] and two different series in NO_3 salt [7]. This complexity arises from a delicate interplay between the anion ordering and SDW nesting. A recent proposition [4] that the frequency of the ROs in Bechgaard salts is proportional to the anion size does not work for ReO_4 and FSO_3 anion salts.

Among the $(TMTSF)_2X$ compounds, the $(TMTSF)_2FSO_3$ salt was expected to exhibit an exceptional difference since asymmetric FSO_3 anions contain permanent electric dipole moments. However, several investigations in the early 1980s [16–19] showed that it had a rather simple pressure–temperature (P–T) phase diagram and exhibited only a featureless, monotonic field dependence in the positive magnetoresistance. As a result, the electronic properties of this salt have remained unexplored.

In this paper, we report observation of the conventional SdH oscillations in the longitudinal magnetoresistance (R_{zz}) of $(TMTSF)_2FSO_3$ under hydrostatic pressure up to 12.8 kbar and at temperatures in the range 0.1–8 K. According to a recent investigation of the phase diagram of $(TMTSF)_2FSO_3$, extraordinary complexity arises between 5 and 9 kbar, where at least four different phases are established between room temperature and 1 K [20]. In this intermediate pressure range, a single series of oscillations with $F_0 = 131 \pm 1$ T, corresponding to about 1.6% of the area of the first Brillouin zone, appears in fields above 5 T. The temperature and field dependence of the oscillation amplitude in this compound fits well to the 2D LK formula adopted by Harrison *et al* [21], indicating the existence of the 2D closed FS in the Q1D $(TMTSF)_2X$ salt. From this LK analysis the effective mass (m_c) and the Dingle temperature (T_D) are estimated as 1.4 ± 0.05 m_0 and 1.6–2.4 K, respectively. The absence of frequency beating, typical in charge transfer salts, indicates that the FS has no detectable warping along the k_z-direction. The pressure effect on the frequency and amplitude of the SdH oscillations, effective mass, and scattering time are discussed within the scope of the new phase diagram suggesting the separation of three different pressure regimes. A sudden change in the electronic properties around 9 kbar gives us a clue for the existence of a new phase under the high pressure.

2. Experiments

$(TMTSF)_2FSO_3$ single crystals were grown by standard electrochemical techniques from TMTSF molecules and tetrabutylammonium-FSO_3. Tiny pieces of crystals about 0.5 mm
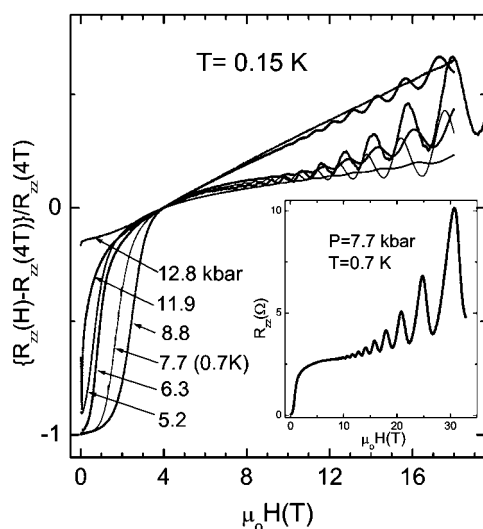
Figure 1. The longitudinal magnetoresistance (R_{zz}) of (TMTSF)$_2$FSO$_3$ at various pressures at 0.15 K (except 0.7 K for 7.7 kbar) with the magnetic field perpendicular to the *ab*-plane. The inset is R_{zz} at 7.7 kbar. There is no sign of a field-induced transition at least up to 33 T.

long were cut from a bar sample and used after checking for the absence of voids. Two 20 μm gold wires were attached to each of the *ab*-planes with silver paste. The samples were mounted in a self-clamped pressure cell so that the *ab*-planes were perpendicular to the magnetic field. Pressure was applied at room temperature using a hydraulic press with a 1:1 mixture of Daphne 7373 oil and kerosene as the pressure medium. The pressure in the cell was measured via the resistance of a manganin pressure gauge next to the sample. The pressures presented here are those at 4.2 K. Pressures at low temperatures were independently calibrated with the superconducting transition of high purity tin. The resistance of samples was measured using the standard lock-in technique with a typical current of 10 μA. The experiments were performed either with a 20 T superconducting magnet at Korea Basic Science Institute in Taejon, Korea or with a 33 T resistive magnet at the National High Magnetic Field Laboratory in Tallahassee, Florida.

3. Results and discussion

Figure 1 shows the low-temperature magnetoresistance at various pressures (5.2, 6.3, 7.7, 8.8, 11.9, and 12.8 kbar) at $T = 0.15$ K (except $T = 0.7$ K for 7.7 kbar). As the magnetic field increases, a series of sinusoidal oscillations appears above 5 T after the superconductivity ($T_c \simeq 3$ K) is destroyed at a critical field. The critical field is highest at 8.8 kbar with a value of 2.5 T, evaluated from the mid-transition field. While the background magnetoresistance increases almost exponentially with the field, the oscillation amplitude monotonically increases to 100% of the background resistance at 33 T, as shown in the inset of figure 1. It is worth pointing out that there is no sign of a field-induced transition at least up to 33 T in the present compound. The absence of the FISDW phases but with the presence of superconductivity is quite exceptional for the (TMTSF)$_2$X salts. This is also counter to Yakovenko's suggestion that the same pairing interaction gives rise to superconductivity at zero field and the FISDW under magnetic field in the Q1D Bechgaard salts [22]. This idea was used to explain the absence
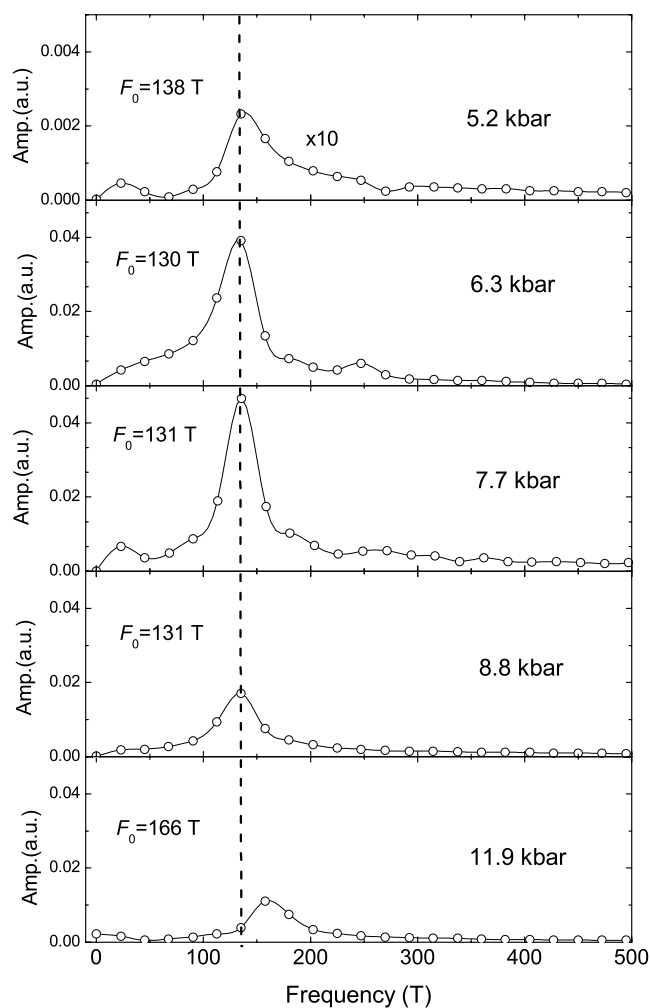
Figure 2. The frequencies and amplitudes of the oscillations in figure 1 are obtained by fast Fourier transform of the oscillatory component subtracting the background magnetoresistance at each pressure.

of both the FISDW and superconductivity in $(TMTSF)_2NO_3$. Hence, the nonexistence of the FISDW states in the presence of the superconductivity indicates that the electronic mechanism of $(TMTSF)_2FSO_3$ under pressure is different from that of other Bechgaard salts.

In figure 1, the field dependence of the background magnetoresistance in the high pressure regime ($P \geqslant 11.9$ kbar) is distinguished from those in the intermediate pressure regime (5 kbar $\leqslant P \leqslant$ 9 kbar). The resistance slope increases from about 0.014 T^{-1} in the intermediate pressure regime to 0.046 T^{-1} in the high pressure regime. The oscillatory behaviour is observable only in pressures between 5.2 and 11.9 kbar, where the ground state is superconducting. The oscillations become visible at 5.2 kbar and have the largest amplitude at 7.7 kbar. However, the oscillations vanish almost completely at 12.8 kbar where the superconductivity is also nearly suppressed.

The fast Fourier transformation spectra for oscillations between 8 and 18 T are shown in figure 2. The oscillation frequencies are 138, 130, 131, 131, 166 and 171 T at 5.2, 6.3, 7.7,
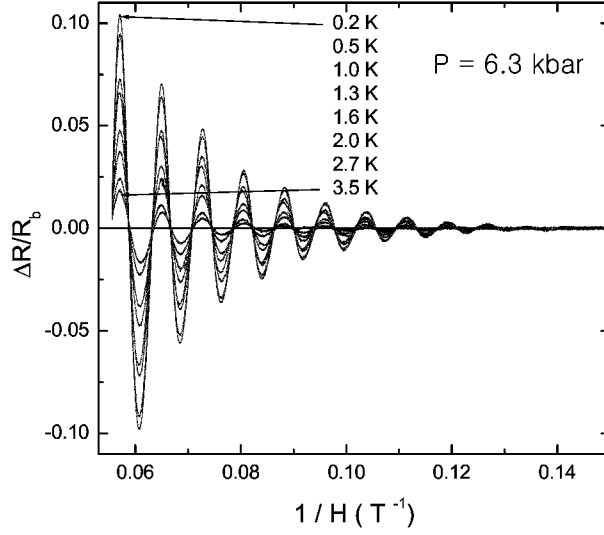
Figure 3. The temperature dependence of the SdH oscillations between 0.1 and 3.5 K at 6.3 kbar.

8.8, 11.9 and 12.8 kbar, respectively. The frequency 171 T at 12.8 kbar was obtained directly from the $1/H$ plot because of the very weak oscillation amplitude. From the frequency of the SdH oscillations, the relevant cross section of the FS S is obtained using the Onsager relation $F = (h/4\pi^2 e)S$. We obtained $S = 1.248 \times 10^{14}$ cm^{-2} for $F_0 = 131$ T, which corresponds to about 1.6% of the first Brillouin zone in the a^*b^*-plane ($S_{FBZ} = 7.6 \times 10^{15}$ cm^{-2}) estimated from the lattice parameters given in [16]. The fundamental frequency is rather insensitive to pressures between 5.2 and 8.8 kbar but increases abruptly by $\sim$30% at 11.9 kbar. It is interesting that, at the same pressure where the fundamental frequency changes, the slope of the background resistance also jumps.

In figure 3, the oscillatory part of the magnetoresistance at 6.3 kbar is plotted as a function of inverse field at several temperatures between 0.2 and 3.2 K. The normalized oscillation amplitude is defined as $\Delta R/R_b = (R - R_b)/R_b$, where R is the overall resistance of the sample and R_b is the non-oscillatory background resistance obtained from polynomial fits. As illustrated in this figure, the oscillation amplitude grows monotonically with decreasing temperature and with increasing field, a typical behaviour of the SdH effects due to the closed orbital motion, but quite unexpected for (TMTSF)$_2$X salts (for example, see figure 3 in [14]). Considering only the first harmonic, the SdH oscillations can be represented by

$$\frac{\Delta R}{R_b} = A_0 \frac{\alpha T \exp(-\alpha m_c/m_0 T_D/H)}{H^q \sinh(\alpha m_c/m_0 T/H)} \cos\left(\frac{F}{H} - \gamma\right) = A \cos\left(\frac{F}{H} - \gamma\right), \quad (1)$$

where $\alpha = 2\pi^2 k_B m_0 c/e\hbar = 14.69$ T K^{-1}, T_D is the Dingle temperature, m_c is the effective mass, and m_0 is the free electron mass. The power of H in equation (1) (the universal LK formula) depends on the dimensionality of the closed motion. For the SdH amplitude in the 2D model q is 1 [23], whereas it is 1/2 in the 3D LK formula [11]. On the other hand, for the 2D dHvA oscillations q becomes 3 [21]. As shown in figure 4(a), the temperature dependence of the amplitude at $H = 16.03$ T for pressures 6.3, 7.7, and 8.8 kbar (symbols) is in remarkably good agreement with the fit (broken lines) to equation (1). The effective mass, which is independent of q, is 1.4 ± 0.05 m_0 and is insensitive to pressure. Once m_c is obtained, T_D can be extracted from the slope of the inverse field dependence of
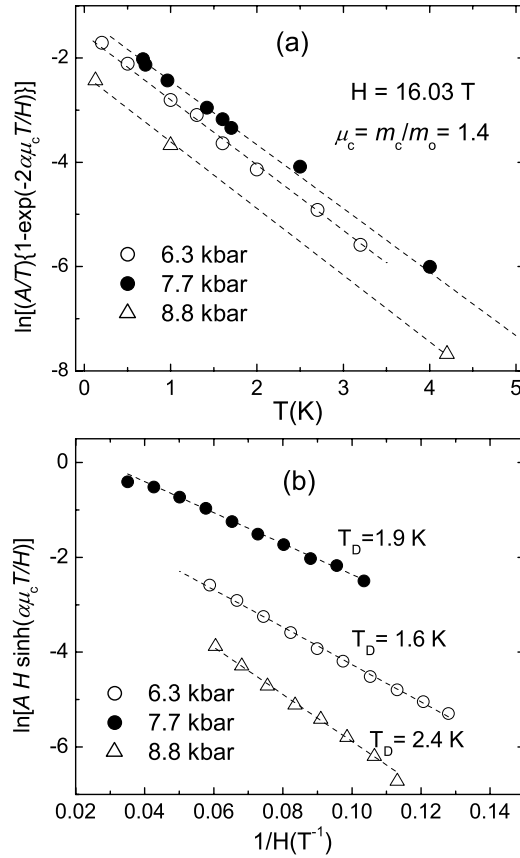
Figure 4. (a) The effective mass (m_c) at pressures of 6.3, 7.7 and 8.8 kbar is estimated as 1.4 m_0 from the temperature dependence of oscillation amplitude. (b) The Dingle plot at $T = 0.1$ K. The data (symbols) are fitted to the theoretical curves by the 2D LK formula (dashed lines).

$\ln[(AH^q)\sinh(\alpha m_c T_{\text{fixed}}/m_0 H)]$, where A is the observed amplitude and q is 1. As our study on angle-dependent magnetoresistance oscillations indicates, the FS of $(TMTSF)_2 FSO_3$ possesses a 2D closed section in the form of a weakly warped cylinder in the same pressure regime [24], therefore it is reasonable to estimate the Dingle temperature through the 2D LK analysis. In figure 4(b) the data (symbols) exhibit very good agreement with the 2D LK formula. The values of T_D ($\propto$relaxation time^{-1}) obtained from this fit are 1.9 K (0.64 ps), 1.6 K (0.76 ps) and 2.4 K (0.5 ps) at 6.3, 7.7 and 8.8 kbar, respectively. The values of T_D with the 3D LK analysis are greater by a factor $\ln\sqrt{2}$ (=0.34). It is worth noting that in the case of α-(BEDT-TTF)$_2$ MHg(SCN)$_4$ (M = NH$_4$ and K), the Dingle plot of the high field SdH [25, 26] and dHvA [23] oscillations deviates from the 3D LK formula and gives a better fit with the 2D model.

It is quite peculiar that the effective mass does not depend upon the applied pressure in the intermediate pressure regime. The effective mass could not be obtained at other pressures (5.2, 11.9 and 12.8 kbar) because of the weak oscillation amplitude even at the lowest temperature, 0.1 K. So, the discussion below is limited to the intermediate pressure regime. In principle, the effective mass derived from the temperature dependence of the SdH amplitude can be considered as $m_c = m_b(1 + \lambda_{e-p})(1 + \lambda_{e-e})$, where m_b is the band mass, λ_{e-p} the electron–phonon interaction and λ_{e-e} the electron–electron interaction [27]. Since m_b
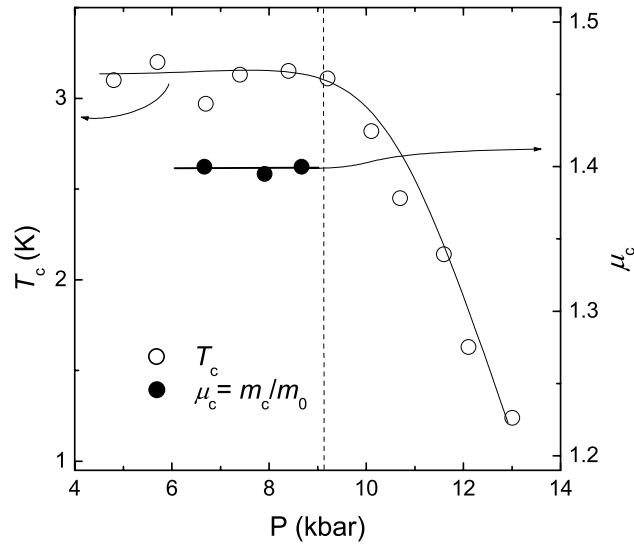
Figure 5. T_c (○) and m_c (●) are plotted as a function of the pressure. m_c is constant where T_c remains unchanged with pressure below 9 kbar.

is virtually pressure-independent, the pressure dependence of m_c provides direct information on the pressure dependence of the interaction terms. As λ_{e-p} also plays an important role on the superconductivity, the pressure dependence of the effective mass provides the relevant information about the superconductivity mechanism in terms of the interactions. Therefore, the insensitivity of the effective mass to the pressure is consistent with the constant T_c in this pressure regime as shown in figure 5.

The pressure dependence of the oscillation amplitude and of the frequency for (TMTSF)$_2$FSO$_3$ is summarized in figure 6(a). The oscillation frequency remains essentially the same from 5.2 to 8.8 kbar, while the amplitude has a maximum in the middle of this same interval, and decreases on each side. Moreover, the pressure dependence of T_D follows that of the amplitudes (i.e., the lower T_D is, the larger the amplitude is). At 11.9 kbar, the oscillation frequency jumps suddenly to 166 T, while its amplitude is continuously reduced after having an abrupt decrease at 8.8 kbar. Then the frequency continues to increase further to 171 T at 12.3 kbar whereas the oscillations disappear almost completely. The abrupt increase of oscillation frequency, discontinuous change of the oscillation amplitude, and the change of slope of the background resistance across 10 kbar may be signs of a pressure induced phase change between intermediate and high pressure regimes.

As is well-known, information on the effective mass for other (TMTSF)$_2$X salts cannot be obtained from the LK theory because of the anomalous temperature and field dependence of the ROs. However, since the oscillations in (TMTSF)$_2$FSO$_3$ are due to 2D closed electron motion, it is reasonable to compare the characteristics of the SdH oscillations with those of the 2D BEDT-TTF salts. According to extensive pressure-dependent studies on α-(BEDT-TTF)$_2$MHg(SCN)$_4$ compounds (M = K, Tl, Rb, and NH$_4$) [27–31] containing both the Q1D open orbit and the Q2D closed orbit, and on κ-(BEDT-TTF)$_2$Cu[N(CN)$_2$]Br [32], the SdH frequency, the effective mass and T_c are highly pressure dependent. The decrease of both T_c and effective mass with pressure in the case of the 10 K superconductor κ-(BEDT-TTF)$_2$Cu(NCS)$_2$ [33] and in α-(BEDT-TTF)$_2$NH$_4$Hg(SCN)$_4$ ($T_c \sim 1$ K) was also explicable using the pressure dependence of the interaction terms.
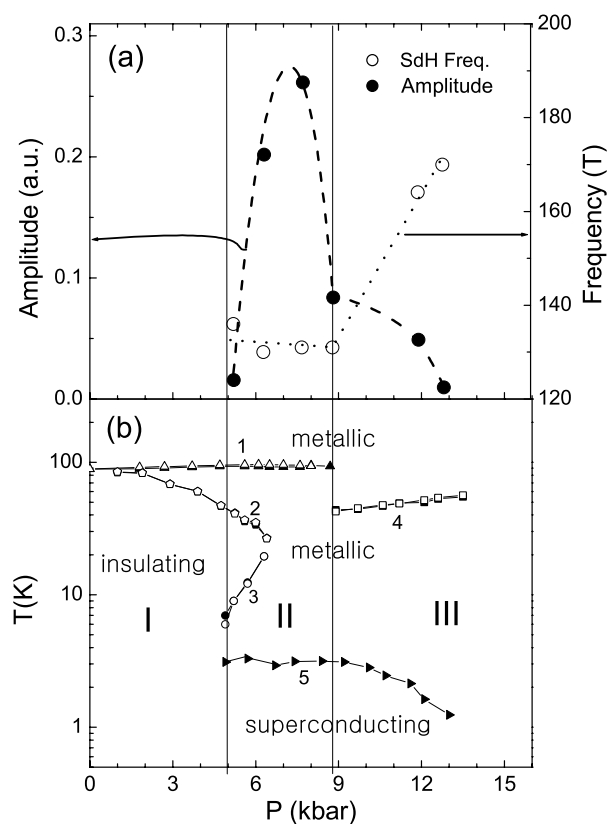
Figure 6. (a) The pressure dependence of the oscillation frequencies (○) and their amplitudes (●). The curves are only guides to the eye. (b) The P–T phase diagram of $(TMTSF)_2FSO_3$ is shown to compare the behaviour of the SdH oscillations with the electronic properties under pressure.

However, the apparent insensitivity of the effective mass, oscillation frequency and interaction parameters in $(TMTSF)_2FSO_3$ to pressure requires a different mechanism. While the BEDT-TTF salts are intrinsically 2D systems, the 2D closed orbit of $(TMTSF)_2FSO_3$ can be formed only through the incomplete nesting of Q1D FS. (It is also assumed that the Q1D FS of the BEDT-TTF salts do the same.) Then, as the real lattice parameters shrink as pressure increases, the cross sectional area of intrinsic 2D FS expands. The 2D closed orbit in $(TMTSF)_2FSO_3$ is not governed directly by the lattice compression but through the change of the best nesting vector. As the pressure changes, so does the best nesting vector so as to maximize the energy gain in such a way that the remaining Q2D FS cross section remains more or less unchanged. In this case, the band mass may or may not depend on pressure. The incomplete nesting scenario can explain the lack of variation of oscillation frequency and of effective mass over quite a wide range of pressure.

To understand the SdH oscillation behaviour with pressure, it is useful to compare the pressure dependence of the SdH oscillations in the context of the refined P–T phase diagram [20] as shown in figure 6(b). Since a detailed explanation of the characteristics of the each phase is well presented in [20], we here discuss only the properties related to SdH oscillations. Due to clear differences in the electric properties, we can divide the pressure into three regimes as follows.

- In pressure regime I (below 5 kbar), neither SdH oscillations nor superconductivity appear. Although the 89 K M–I transition at ambient pressure splits into two discrete transitions as pressure is applied, the low-temperature state is still insulating up to 5 kbar.

- In the pressure range between 5 and 9 kbar, denoted as pressure regime II in figures 6(a) and (b), the material remains metallic at low temperature and the superconducting transition occurs at $\sim$3 K. T_c is more or less constant regardless of the normal state resistance which varies over three orders of magnitude. The conventional SdH oscillations of frequency $\sim$130 T observed in this pressure regime confirm the existence of a Q2D closed orbit of 1.6% of S_{FBZ} in this regime. As discussed earlier, the constancy of the effective mass, of the SdH frequency, and of T_c is due to the adjustment of the nesting condition of FS at this pressure.

- As the pressure increases above 9 kbar (pressure regime III in figure 6), the characteristics of the SdH oscillations, such as the frequency and amplitude, suddenly change. Here, the superconducting transition is rapidly suppressed at a rate of $dT_c/dP \simeq -0.5$ K kbar^{-1}. Moreover, the different field dependence of the background resistance (as seen in figure 1) also indicates that the electronic mechanism in pressure regime III is different from that in pressure regime II. It is possible that the new transition around 50 K (line 4 in figure 6(b)) in regime III is due to a new kind of anion ordering as the pressure increases above 9 kbar.

4. Summary

In summary, the pressure dependence of the magnetoresistance and the SdH oscillations leads to a new phase diagram for the Bechgaard salt (TMTSF)$_2$FSO$_3$. We observe conventional SdH oscillations in this salt between 5.2 and 12.8 kbar. Quite striking is that the oscillations can be analyzed in terms of the archetypal 2D closed electronic motion, unlike those in most (TMTSF)$_2$X salts. A closed orbit can be formed by an imperfect nesting of FS under pressure. It is also possible to consider that a separated ordering between the structural and dipole ordering of FSO$_3$ anions may occur and leave the small closed orbit on FS as the temperature decreases. The superconductivity with high T_c, the absence of the FISDW, and the SdH oscillations result from the same electrons on this small closed pocket. In particular, the pressure dependence is divided into three different regimes as shown in figure 6, according to the characteristics of the SdH oscillations as well as electronic properties. Systematic studies such as x-ray diffraction analysis, electron spin resonance, and anisotropic susceptibility measurements under pressure are necessary to correlate these phenomena.

Acknowledgments

References

[1] For a review, see Ishiguro T and Yamaji K 1998 *Organic Superconductors* 2nd edn (Berlin: Springer)
  Wosnitza J 1996 *Fermi Surface of Low-Dimensional Organic Metals* (Berlin: Springer)
[2] Ulmet J P, Auban P, Khmou A and Askenazy S 1985 *J. Physique Lett.* **46** L535
[3] Audouard A, Ulmet J P and Fabre J M 1995 *Synth. Met.* **70** 751
[4] Vignolles D, Ulmet J P, Naughton M J, Binet L and Fabre J M 1998 *Phys. Rev.* B **58** 14476
[5] Ulmet J P, Khmou A, Auban P and Bachere L 1986 *Solid State Commun.* **58** 753
  Yan X, Naughton M J, Chamberlin R V, Hsu S Y, Chiang L Y, Brooks J S and Chaikin P M 1989 *Phys. Rev.* B **36** 1799

[6] Schwenk H, Parkin S S, Schumarker R, Green R L and Schweitzer D 1986 *Phys. Rev. Lett.* **56** 667
Kang W, Cooper J R and Jeróme D 1991 *Phys. Rev.* B **43** 11467

[7] Kang W, Hannahs S T, Chiang L Y, Upasani R and Chaikin P M 1990 *Phys. Rev. Lett.* **65** 2812
Audouard A, Goze F, Dubois S, Ulmet J P, Brossard L, Askenazy S, Tomic S and Fabre J M 1994 *Europhys. Lett.* **25** 363
Audouard A, Goze F, Dubois S, Ulmet J P, Brossard L, Askenazy S, Tomic S and Fabre J M 1995 *Synth. Met.* **70** 739
Audouard A, Goze F, Dubois S, Ulmet J P, Brossard L, Askenazy S, Tomic S and Fabre J M 1995 *Physica* B **211** 303
Kang W, Balicas L, Behnia K, Jeróme D, Ribault M and Fabre J M 1995 *Synth. Met.* **70** 755

[8] Gorkov L P and Lebed A G 1984 *J. Physique Lett.* **45** L433

[9] Montambaux G, Heritier M and Lederer P 1984 *J. Physique Lett.* **45** L533
Chaikin P M 1985 *Phys. Rev.* B **31** 4770
Azbel M Ya, Bak P and Chaikin P M 1986 *Phys. Lett.* A **117** 92
Maki K 1986 *Phys. Rev.* B **33** 4826

[10] Lifshitz I M and Kosevich A M 1944 *Zh. Eksp. Teor. Fiz.* **29** 730
Lifshitz I M and Kosevich A M 1956 *Sov. Phys.—JETP* **2** 636 (Engl. Transl.)

[11] Shoenberg D 1984 *Magnetic Oscillations in Metals* (Cambridge: Cambridge University Press)

[12] Brooks J S *et al* 1996 *Phys. Rev.* B **53** 14406

[13] Uji S, Terashima T, Aoki H, Brooks J S, Tokumoto M, Takasaki S, Yamada J and Anzai H 1996 *Phys. Rev.* B **53** 14399

[14] Chung O H, Kang W, Kim D L and Choi C H 2000 *Phys. Rev.* B **61** 11649

[15] Uji S, Brooks J S, Chaparala M, Takasaki S, Yamada J and Anzai H 1997 *Phys. Rev.* B **55** 12446

[16] Wudl F *et al* 1982 *J. Chem. Phys.* **76** 5497

[17] Lacoe R C, Wolf S A, Chaikin P M, Wudl F and Aharon-Shalom E 1983 *Phys. Rev.* B **27** 1947

[18] Lacoe R C, Chaikin P M, Wudl F and Aharon-Shalom E 1983 *J. Physique Coll.* **44** C3 767

[19] Gross F, Schwenk H, Andres K, Wudl F, Cox S D and Brennan J 1984 *Phys. Rev.* B **30** 1282

[20] Jo Y J, Choi E S, Kang H, Kang W, Seo I S and Chung O H 2003 *Phys. Rev.* B **67** 014516

[21] Harrison N, House A, Deckers I, Caulfield J, Singleton J, Herlach F, Hayes W, Kurmoo M and Day P 1995 *Phys. Rev.* B **52** 5584
Harrison N, Bogaerts R, Reinders P H P, Singleton J, Blundell S J and Herlach F P 1996 *Phys. Rev.* B **54** 977

[22] Yakovenko V M 1987 *Zh. Eksp. Theor. Fiz.* **93** 627
Yakovenko V M 1987 *Sov. Phys.—JETP* **66** 355 (Engl. Transl.)

[23] Ivanov S A, Mielke C H, Coffey T, Howe D A, Agosta C C, Fravel B W and Montgomery L K 1997 *Phys. Rev.* B **55** 4191

[24] Kang W, Chung O H, Jo Y J, Kang H Y and Seo I S 2003 *Phys. Rev.* B **68** 073101

[25] Sandhu P S, Athas G J, Brooks J S, Haanappel E G, Goettee J D, Rickel D W, Tokumoto M, Kinoshita N, Kinoshita T and Tanaka Y 1996 *Surf. Sci.* **361/362** 913

[26] Caulfield J *et al* 1995 *Phys. Rev.* B **51** 8325

[27] Brooks J S *et al* 1995 *Phys. Rev.* B **52** 14457

[28] Klepper S J, Brooks J S, Chen X, Bradaric I, Tokumoto M, Kinoshita N, Tanaka Y and Agosta C C 1993 *Phys. Rev.* B **48** 9913

[29] House A A, Lubczynski W, Blundell S J, Singleton J, Hayes W, Kurmoo M and Day P 1996 *J. Phys.: Condens. Matter* **8** 10377

[30] Sasaki T, Toyota N, Tokumoto M, Kinoshita N and Anzai H 1990 *Solid State Commun.* **75** 93

[31] Schegolev A I, Laukin V N, Khomenko A G, Kartsovnik M V, Shivaeva R P, Rozenberg L P and Kovalev A E 1992 *J. Physique* I **2** 2123

[32] Weiss H, Kartsovnik M V, Biberacher W, Steep E, Balthes E, Jansen A G M, Andres K and Kushch N D 1999 *Phys. Rev.* B **59** 12370

[33] Caulfield J, Lubczynski W, Pratt F L, Singleton J, Ko D Y, Hayes W, Kurmoo M and Day P 1994 *J. Phys.: Condens. Matter* **6** 2911